



Technical Memorandum--86192

(NASA-TM-86192) EVOLUTION AND INTERACTION
OF LARGE INTERPLANETARY STREAMS (NASA) 41 p
CSCL 54C

N87-15131

Unclas

G3/90 43674

EVOLUTION AND INTERACTION OF LARGE INTERPLANETARY STREAMS

Y. C. Whang
L. F. Burlaga

FEBRUARY 1985

National Aeronautics and
Space Administration

Goddard Space Flight Center
Greenbelt, Maryland 20771



EVOLUTION AND INTERACTION OF LARGE INTERPLANETARY STREAMS

Y. C. Whang

Department of Mechanical Engineering

Catholic University of America

Washington, D.C.

L. F. Burlaga

Laboratory for Extraterrestrial Physics

NASA-Goddard Space Flight Center

Greenbelt, Maryland

February 8, 1985

Short title: Evolution of large streams

Submitted to the Journal of Geophysical Research

Abstract. The paper presents a computer simulation for the evolution and interaction of large interplanetary streams based on multi-spacecraft observations and an unsteady, one-dimensional MHD model. We studied two events each observed by two or more spacecraft separated by a distance of the order of 10 AU. The first simulation is based on the plasma and magnetic field observations made by two radially-aligned spacecraft: first by IMP-8 in November 1977 at 1 AU, and later by Pioneer-10 in January 1978 at 15 AU. The second simulation is based on an event observed first by Helios-1 in May 1980 near 0.6 AU and later by Voyager-1 in June 1980 at 8.1 AU. These examples show that the dynamical evolution of large-scale solar wind structures is dominated by the shock process, including the formation, collision and merging of shocks. Formation of shocks continues to take place even outside 5 AU. Collision and merging of shocks irreversibly restructure the solar wind. The interaction of shocks with stream structures also causes a drastic decrease in the amplitude of the solar wind speed variation with increasing heliocentric distance, and as a result of interactions there is a large variation of shock-strengths and shock-speeds. In the outer heliosphere, the large-scale solar wind and magnetic field evolve into a much simpler structure and MHD shocks are present as a principal component of the solar wind. The simulation results shed new light on interpretation for the interaction and evolution of large interplanetary streams. Observations were made only along a few limited trajectories, but simulation results can supplement these by providing the detailed evolution process for large-scale solar wind structures in the vast region not directly

observed. The use of a quantitative nonlinear simulation model including shock merging process is crucial in the interpretation of data obtained in the outer heliosphere.

1. Introduction

This paper presents a computer simulation for the evolution and interaction of large interplanetary streams based on multi-spacecraft observations and an unsteady, one-dimensional MHD model. We studied two events each observed by two spacecraft separated by a distance of the order of 10 AU. The first simulation study is based on the plasma and magnetic field observations made by two radially-aligned spacecraft: IMP-8 in November 1977 at 1 AU, and Pioneer-10 in January 1978 at 15 AU. The second is based on the event first observed by Helios-1 in May 1980 near 0.6 AU, and later by Voyager-1 in June 1980 at 8.1 AU. We have found good agreement between model and observational data.

It is well established that the evolution of a single high-speed stream near or outside 1 AU leads to the formation of a forward-reverse shock pair [Dessler and Fejer, 1963; Hundhausen and Gosling, 1976]. Hundhausen and Gosling showed that at large heliocentric distances, the shock pair evolves into a double-sawtooth velocity profile similar to that observed by Pioneer 10. Their calculation also shows a large enhancement in plasma density in the compression region bounded by the shock pair. An analysis of Pioneer 10 and 11 magnetic field and plasma observations by Smith and Wolfe [1976] reported the observation of large enhancements in density, temperature, field strength, and fluctuation level in the interaction regions bounded by the shock pairs.

The forward and the reverse shock propagate in opposite directions in a frame of reference moving with the solar wind and

interact with the stream structures. At large heliocentric distances, shocks belonging to neighboring streams also interact with one another. In addition to the interaction of a shock with the stream structure, collision of a forward and a reverse shock and merging of two forward or two reverse shocks may take place. These interactions play very important roles on the dynamical evolution of large-scale interplanetary structures. They can significantly modifies the structure of the solar wind.

The evolution process of large-scale interplanetary structures has been discussed by Gosling et al. [1976], Burlaga et al. [1983], Burlaga [1983], and Burlaga and Goldstein [1984], and they were reviewed by Burlaga [1985]. Dryer and Steinolfson [1976], Dryer et al. [1978] and Whang and Burlaga [1985] have calculated the collision between the forward and reverse shocks from adjacent shock pairs. Burlaga [1983] estimated that at 20-25 AU shocks from successive solar rotations have had time to propagate all the way across the intervening structures and meet, and this was confirmed by numerical calculations based on a corotating MHD model [Pizzo, 1983]. Thus at those distances the entire flow should have been shocked at least once.

Numerical simulations for interplanetary shocks have been studied using two approaches: unsteady one-dimensional models [Hundhausen, 1973a,b; Steinolfson et al., 1975; and Whang, 1984]; and quasi-steady corotating models [Pizzo, 1978, 1980, 1982; Whang and Chien, 1981]. In this paper, we use Whang's unsteady one-dimensional MHD model to carry out a simulation study for the evolution of the solar wind over a distance of the order of 10 AU

in the outer heliosphere.

2. Simulation Model

The model assumes that the physical properties near the equatorial plane are functions of the time t and the heliocentric distance r only: the flow is radial and the magnetic field is azimuthal. The method of solution uses the shock surfaces to divide the domain of solutions in the t, r -plane into several continuous flow regions. In each region, the governing equations for the flow field can be integrated along three special directions in the t, r -plane. The "initial" conditions are given as functions of t at a given heliocentric distance. They are generated from observed plasma data and the non-radial components of observed magnetic field data.

Let u denote the solar wind speed, B the non-radial component of the magnetic field, p the thermal pressure, ρ the plasma density, p^* the total pressure (sum of the thermal and the magnetic pressure), a the Alfvén speed, c the gasdynamic sound speed, G the gravitational constant, and M the mass of the sun. Along the path of each fluid element defined by $dr/dt = u$ in the continuous flow region, we have

$$B / \rho r = \text{constant}$$

and

$$p \rho^{-5/3} = \text{constant}.$$

Along the two characteristic directions defined by $dr/dt = u \pm C_f$, we have

$$\left(\frac{\partial p^*}{\partial t} \right)_{\pm} \pm \rho C_f \left(\frac{\partial u}{\partial t} \right)_{\pm} = s_{\pm}$$

where $C_f = (c^2 + a^2)^{1/2}$ is the fast speed,

and

$$\left(\frac{\partial}{\partial t} \right)_{\pm} = \frac{\partial}{\partial t} + (u \pm C_f) \frac{\partial}{\partial r}$$

$$s_{\pm} = \frac{\rho}{r} \left[a^2(u \mp C_f) \mp C_f \frac{GM}{r} - 2u C_f^2 \right]$$

A detailed discussion of these equations and the method of numerical integration can be found in Whang [1984].

We treat shocks as surfaces of discontinuity with zero thickness. The jump conditions of MHD shocks describe the flow conditions across the boundaries between flow regions. At grid points on the shock boundary each flow variable has two values: the conditions on the front and on the back side of the shock. The plasma enters the shock from the front side and exits on the back side. For interaction problems, two or more shock surfaces are present in the region where collision or merging of shocks takes place. This method of solutions allows a flexible adjustment of the grid sizes, so that a reasonable number of grid points can be maintained in order to attain a meaningful description for the detailed dynamical structure of the flow field.

3. Multi-spacecraft Observation of November 1977 Stream Interaction

In a three months period starting November 1977 four spacecraft (IMP-8, Voyager 1, Voyager 2, and Pioneer 10) were nearly radially-aligned at different times following the motion of the solar wind. The same solar wind were observed at different heliocentric distances by these spacecraft: by IMP-8 at 1 AU, by Voyagers at near 1.5 AU, and by Pioneer-10 at 15.1 AU. Figure 1 shows the relative positions of the three spacecraft with reference to IMP-8. The relative positions were calculated using an average solar wind speed of 0.22 AU/day. The solar wind observed by the spacecraft (SC = Voyager-1,2 or Pioneer-10) at heliocentric distance r_{sc} and time t_{sc} was at 1 AU, the heliocentric distance of IMP-8, at time t_{imp8} with

$$r_{sc} - r_{imp8} = 0.22 * (t_{sc} - t_{imp8}).$$

The positions of spacecraft in the inertial heliographic coordinates X,Y,Z are shown in Figure 1 in terms of the heliolongitude ϕ and the heliolatitude θ defined by

$$\tan \phi = -Y / X$$
$$\tan \theta = Z / (X^2 + Y^2)^{1/2}.$$

Here, the X,Y-coordinate plane is the sun's equatorial plane, X-axis in the direction of sun's vernal equinox, and Z in the direction of sun's north heliographic pole. The three spacecraft and IMP-8 were less than 15 degrees apart in longitude and within 5 degrees in latitude. These almost radially-aligned spacecraft have observed the solar wind separated by a distance of 14 AU following its radial motion. Their observations provide a rare opportunity to study the evolution of the solar wind in the outer

heliosphere. Observational data of plasma and magnetic field from IMP-8 at 1 AU are used as input for our simulation.

Figure 2 shows the hourly averages of the solar wind speed observed by IMP-8, Voyager-1, and Pioneer-10. Three large streams (A, B and C) were observed by IMP-8 at 1 AU and by Voyagers near 1.5 AU. The variation of the solar wind speeds of these streams has an amplitude of the order of 300 km/s. This solar wind was observed by Pioneer-10 at 15.1 AU as a distinctly different structure, and as expected no traces of the streams survived [Collard et al., 1982]; the amplitudes of the solar wind speed variation were reduced to less than 50 km/s. The only significant solar wind structures that can be identified from the plasma data at 15.1 AU are four shock waves arranged in a F-R-F-R sequence (F for forward shock and R for reverse shock). We identify these shocks as FB, RA, FC, and RB in Figure 2. As discussed below, the result of this simulation study explains that the first and the fourth of the shocks sequence shown on the top panel of Figure 1, FB and RB, are members of the pair of forward-reverse shocks originally formed at the leading edge of the stream B. The two shocks between FB and RB are respectively associated with the two neighboring streams: RA is the remnant of reverse shock associated with the stream A, and FC the forward shock associated with the stream C.

Stream B (shown in Figure 2) has been discussed by Burlaga et al. [1984b], who examined its evolution from 1 AU to 4 AU using a stationary, two-dimensional MHD model for corotating streams based on a finite difference code in which shocks are treated by

means of artificial viscosity [Pizzo, 1982]. Their study compared results of the model with observations made by Voyager 1 at 1.5 AU. In this study we compare the simulation results with observations made near 15.1 AU by Pioneer-10 (see the top panel of Figure 2). This simulation uses a characteristics code based on a unsteady, one-dimensional MHD model in which shocks are treated as discontinuity surfaces. It will be shown that the evolution of stream B out to 15 AU is influenced by the streams ahead of and behind it, and for this reason we consider streams A and C as well as stream B.

4. Simulation of November 1977 Event

Hourly averages of the plasma and magnetic field data from IMP-8 are used to generate the initial condition for the simulation of the the evolution process. We assume that the electron and the proton pressure are equal. Smooth curves are used to represent the data points. The curve fitting procedure is carried out in the logarithmic scale plots for the field magnitude, the number density, and the total pressure, and in the linear scale plots for the solar wind speed.

The leading edge of stream B has a complicated structure near 1 AU. On the one hand, it is a "compound stream", according to the classification of Burlaga [1975], made up of two streams of different origins, having opposite magnetic field polarities, two stream interfaces and two interaction regions (see the discussion in Burlaga et al. 1984b). On the basis of earlier studies, one anticipates that two shock pairs will tend to develop ahead of stream B, one from each interaction region. On the other hand, one can also see "irregular variations" in the speed profile. Burlaga [1975] suggested that these speed variations might be significantly altered by pressure gradients when the change in solar wind speed is less than the magnetoacoustic speed. Gosling et al. [1976] suggested the fluctuations in speed would give rise to shock pairs and thereby "damp-out". Since the main thrust of this paper is to study the evolution of large-scale streams over a distance of the order of 10 AU, the smoothed input function does not contain small "irregular variations" present in the initial data.

The formation of a forward-reverse shock pair at the leading

edge region of a real stream involves a rather complicated process. Figure 3 shows the computed profiles of the solar wind speed (the t,u -profiles) at the leading edge of stream B between 1 AU and 3 AU at increments of 0.04 AU. Shock formation tends to occur at locations where the flow speed increases rapidly. While stream B moved outward in interplanetary space between 1.5 AU and 3 AU, at least three shocks were present simultaneously at its leading edge region in this simulation. Two of the three shocks predicted by the model at 1.5 AU were observed by Voyager 1 [Burlaga et al., 1984b, Figure 10], but the third shock (a reverse shock) was not fully developed. Collision and merging process also took place during the complicated formation process of a shock pair at the leading edge of stream B. A forward and a reverse shock collided near the center of the leading edge at about 2 AU. Three reverse shocks merged near 2.5 AU, and formed a single reverse shock RB, the final reverse shock associated with stream B. The net result of the evolution of stream B out to 3 AU is the presence of two forward shocks and a reverse shock RB. Later on the two forward shocks also merged, and the leading edge region of stream B finally evolved into a simple shock pair (FB and RB) by 4 AU. The pair continue to move outwards and eventually interacted with shocks associated with the neighboring streams.

The flow speed profiles and the total pressure profiles in Figure 4 show the evolution of stream B and its interaction with neighboring streams A and C. The input data at 1 AU are plotted on the two bottom panels. At 4 AU stream B evolved into a

single interaction region bounded by a forward-reverse shock pair. This is in agreement with the results of Pizzo's code [Burlaga et al., 1984b, Figure 11]. The interaction regions associated with streams A and C also had a simple form at 4 AU, each bounded by a forward-reverse shock pair, and the streams had evolved into the familiar sawtooth profiles at 4 AU.

Beyond 4 AU each interaction region, which may be regarded as a pressure wave, expanded as its two boundaries propagated in the solar wind frame in opposite directions. The interaction regions associated with stream B and C merged at 9.52 AU, as shock FC collided with RB, and a "secondary interaction region" was formed as part of a broad "merged interaction region". Similarly, the interaction regions associated with streams A and B merged at 11.43 AU as shock FB collided with shock RA, and another "secondary interaction region" was formed. Thus at 13 AU, all the plasma was shocked at least once, and some of the plasma in the secondary interaction regions was shocked twice.

As a result of the collisions between a forward shock and a reverse shock, a contact surface appeared in the secondary interaction region. Across the contact surface the temperature, the number density, and the field magnitude are discontinuous, but the solar wind speed and the total pressure are continuous. From t, p^* -profiles, one can unmistakably identify whether a surface of discontinuity is a forward shock, a reverse shock or a contact surface. The contact surfaces do not play important roles in the dynamical processes considered here.

Figure 5 plots the calculated trajectories of shocks in a frame of reference moving at a speed of 0.22 AU/day. It shows the

time and the heliocentric distance at which each collision or merging of shock waves took place. The plot indicates that a sequence of shocks (FB-RA-FC-RB) should pass a radially-aligned spacecraft at 15 AU from January 4 to January 30, 1978. Thus, it explains the relationship between the sequence of shocks observed by Pioneer-10 and the large interplanetary streams observed by IMP-8. This simulation result, based on the event observed first by IMP-8 in November 1977 at 1 AU and later by Pioneer-10 in January 1978 at 15.1 AU, shows good agreement between model and observational data, the error in the shock arrival times at Pioneer-10 being less than 10%. Observations can be made only along a few limited trajectories, but computer simulation can supplement these by providing the detailed information on the evolution and interaction of large-scale interplanetary streams in the vast unobserved region between the various spacecraft.

The evolution of a shock in interplanetary space may be described by the variation of its shock-strength and shock-speed. The strength of a shock may be represented by the density ratio or the total pressure ratio across the shock. The speed of a reverse shock seen in an inertial system increases as its strength decreases, whereas the speed of a forward shock increases as its strength increases. In figure 6 we use shock RB, described in Figures 3 and 5, as an example to illustrate how the state of a reverse shock may vary as it moves from 1 AU to 16 AU in 85 days. The shock strength grows rapidly during the initial formation process inside 2 AU. The reverse shock was weakened by its collision with a forward shock at 2.03 AU, and there was a

corresponding sudden increase in shock speed. Its strength continued to grow as RB merged with three other reverse shocks between 2.4 AU and 4 AU. Its strength dropped near 9.52 AU after colliding with FC. Near 14.5 AU, the shock interacted with a contact surface, but the interaction produced a relatively insignificant effect on the global evolution of the stream structure.

5. Stream Interactions of May 1980

The second simulation uses the solar wind and magnetic field data obtained by Helios-1 near 0.6 AU in May 1980 as input, and it compares the resulting output of the model with the observations made from Voyager-1 at 8.1 AU in June 1980. Figure 7 shows the hourly averages of the solar wind speed observed from the two spacecraft. Three large streams (A, B and C) were observed by Helios-1 near 0.6 AU. As discussed by Burlaga et al. [1984b] these were corotating streams, and each of these streams was preceded by a shock pair [Volkmer and Neubauer 1984]. Voyager-1 found the corresponding solar wind structure at 8.1 AU to consist of four shock waves arranged in a F-F-R-R sequence. Burlaga [1985] suggested that a shock pair formed ahead of each of streams B and C, and that the shocks interacted to form a merged interaction region with the signature of F-F-R-R. We shall show that this process take place between 0.6 AU and 4.6 AU, but further interactions occur beyond 4.6 AU such that the F-F-R-R signature observed by Voyage-1 has a more complex history.

The hourly averages of the plasma and magnetic fields data observed from Helios-1 in May 1980 are used as the input function for this simulation study. During this period, the heliocentric distances of the spacecraft's trajectory varied between 0.4 AU and 0.8 AU as shown in Figure 8 of Burlaga et al. [1984a]. When the observational data were used as the input function at 0.6 AU, we made some adjustments of the initial conditions by assuming the following relations for the variation of the proton number density, the temperature, and the non-radial component of the magnetic field as functions of the heliocentric distance r :

$$n r^2 = \text{constant},$$

$$T r^{2/5} = \text{constant},$$

and

$$B r = \text{constant}.$$

No adjustment was made for the solar wind speed. The simulation result explains what is likely to have taken place between the two observations. The input data were smoothed as described above, so again the small irregular variations are not included in the input function, and the simulation exhibits only the large-scale behavior of the evolution process. The relative positions of Voyager-1 with reference to Helios-1 calculated using an average solar wind speed of 0.22 AU/day show that

$$-50 \text{ degrees} < \phi_{\text{voy1}} - \phi_{\text{helios1}} < -10 \text{ degrees}$$

and

$$0.2 \text{ degrees} < \theta_{\text{voy1}} - \theta_{\text{helios1}} < 2.2 \text{ degrees}.$$

If the solar wind structure was quasi-steady during that period, then Voyager-1 should have seen the same solar wind about two days before the observation of this wind by a perfectly radially-aligned spacecraft.

The formation and interaction of the forward-reverse shock pairs at the leading edge regions of the three streams A, B, and C again involves a series of complicated processes. Figure 8 shows the profiles of the solar wind speed (the t, u -profiles) between 0.6 AU and 8.1 AU at increments of 0.1 AU. This detailed plot shows that several formation, merging and collision processes took place during the evolution of the interplanetary structure studied by this simulation.

Let us first examine the evolution of the the streams B and C.

Two shock pairs were produced at the leading edges of the streams: FB and RB identify the forward and reverse shocks associated with stream B, and FC and RC identify the shocks with stream C. The collision of RB with FC took place at 1.93 AU. The two reverse shocks RB and RC merged at 4.64 AU to form a single reverse shock RBC. Thus, a spacecraft between 2 AU and 4.6 AU would have observed the signature of a shocks sequence F-F-R-R as a result of the interaction between streams B and C. The signature F-F-R-R was also observed by Voyager-1, but our simulation shows that this has a more complex history, involving the nonlinear interaction of three neighboring streams A, B, and C.

The two forward shocks FB and FC propagated outward and were observed by Voyager-1 at 8.1 AU, as indicated in Figure 7. However these shocks were modified by their collisions with a reverse shock RA associated with stream A. As the reverse shock RA of the pair associated with stream A propagated outward in the region between 1 AU and 5 AU, the stream structure initially about 5 days ahead of stream A gradually evolved to form a new reverse shock near 4 AU. RA merged with this new shock to form a stronger reverse shock. This modified RA continued to propagate outward, and it eventually collided with FB at 6.98 AU and with FC at 7.75 AU. The strength of shock RA was substantially weakened by the two consecutive collisions. Our simulation result suggested that the sequence F-F-R-R observed by Voyager-1 at 8.1 AU consists of FB, FC, RA, and RBC. Voyager-1 observed the three shocks FB and FC soon after their collisions with RA, that is before the solar wind structure had enough time to evolve into a

new sawtooth configuration. The reverse shock RBC was further strengthened as it interacted with a nonlinear wave structure near 6.4 AU before RBC was observed by Voyager-1.

This simulation provides a striking illustration of the irreversibility of the nonlinear interactions that can occur in the outer heliosphere. It shows a specific mechanism for the increase in entropy in the system. The same signature, such as F-F-R-R can be produced in more than one way as shown above. Thus, the mapping from the inner heliosphere to the outer heliosphere can be a many mapping which is irreversible. The use of a quantitative nonlinear simulation model including shock merging process is crucial in the interpretation of data obtained in the outer heliosphere, because the mappings are nonlinear and not necessarily one to one.

The flow speed profiles and the total pressure profiles (Figure 9) show the evolution of the interplanetary dynamical structure for the interaction of the three streams A, B, and C. Each merging or collision creates a significant change in the profiles of the total pressure. Due to the proximity of the two streams, the interaction regions of streams B and C coalesced very rapidly. By 2.1 AU they have already begun to interact and a secondary interaction region has formed. At 8.1 AU the interaction region associated with stream A has coalesced with the interaction region of streams B and C.

Figure 10 plots the calculated trajectories of shocks in a frame of reference moving at a speed of 0.22 AU/day. It shows the time and the heliocentric distance at which each collision or

merging of two shock waves took place, and it provides a summary of all the interactions out to 8.1 AU. Note that the merging of two shocks is represented by a triple-junction and the collision of two shocks moving in opposite directions is represented by a junction with four lines at a point. The plot explains the relationship between the sequence of shocks observed by Voyager-1 and the large interplanetary streams observed by Helios-1. The times at which the shocks were observed by Voyager-1 agree within 10% with those computed from the Helios-1 observations. Evolution of the stream structures over a distance of the order of 10 AU is definitely a complicated process, but this complexity is not without some order. MHD shocks and their interactions play very important roles in partitioning and restructuring the heliosphere. Figures 5 and 10 present a clear display of the complex nature of the evolution process.

Acknowledgments. We are grateful to H. Bridge and A. Lazarus for allowing us to use their plasma data from Voyager 1 and 2, to H. Rosenbauer and R. Schwenn for plasma data from Helios-1, to N. Ness for magnetic field data from Voyager 1 and 2, and to F. Mariani for magnetic field data from Helios-1.

References

- Burlaga, L. F., A reverse hydromagnetic shock in the solar wind, Cosmic Electrodynamics, 1, 233, 1970.
- Burlaga, L. Interplanetary streams and their interaction with the earth, Space Sci. Rev., 17, 327, 1975.
- Burlaga, L. F., Corotating pressure waves without fast streams in the solar wind, J. Geophys. Res., 88, 6085, 1983.
- Burlaga, L. F., R. Schwenn, and H. Rosenbauer, Dynamical evolution of interplanetary magnetic fields and flows between 0.3 AU and 8.5 AU: Entrainment, Geophys. Res. Lett., 10, 413, 1983.
- Burlaga, L. F., and M. L. Goldstein, Radial variations of large-scale magnetohydrodynamic fluctuations in the solar wind, J. Geophys. Res., 89, 6813, 1984.
- Burlaga, L. F., F. B. McDonald, N. F. Ness, R. Schwenn, A. J. Lazarus, and F. Mariani, Interplanetary flow systems associated with cosmic ray modulation in 1977-1980, J. Geophys. Res., 89, 6579, 1984a.
- Burlaga, L., V. Pizzo, A. Lazarus, and P. Gazis, Stream dynamics between 1 AU and 2 AU: a detailed comparison of observations and theory, NASA TM, 86086, 1984b.
- Burlaga, L., MHD processes in the outer heliosphere, Space Sci. Rev., in press, 1985.
- Collard, H. R., J. D. Mihalov and J. H. Wolfe, Radial variation of the solar wind speed between 1 and 15 AU, J. Geophys. Res., 87, 2203, 1982.
- Dessler, A. J., and J. A. Fejer, Interpretation of Kp index and M-region geomagnetic storms, Planet. Space Sci., 11, 505, 1963.

Dryer, M., and R. S. Steinolfson, MHD solution of interplanetary disturbances generated by simulated velocity perturbations, J. Geophys. Res., 81, 5413, 1976.

Dryer, M., Z. K. Smith, E. J. Smith, J. D. Mihalov, J. H. Wolfe, R. S. Steinolfson, and S. T. Wu, Dynamic MHD modelling of solar wind corotating stream interaction regions observed by Pioneer 10 and 11, J. Geophys. Res., 83, 4347, 1978.

Gosling, J. T., A. J. Hundhausen, and S. J. Bame, Solar wind stream evolution at large heliocentric distances, J. Geophys. Res., 81, 2111, 1976.

Hundhausen, A. J., Nonlinear model of high-speed solar wind streams, J. Geophys. Res., 78, 1528, 1973a.

Hundhausen, A. J., Evolution of large-scale solar wind structures beyond 1 AU, J. Geophys. Res., 78, 2035, 1973b.

Hundhausen, A. J., and J. T. Gosling, Solar wind structures at large heliocentric distances: An interpretation of Pioneer 10 observations, J. Geophys. Res., 81, 1436, 1976.

Pizzo, V. J., A three-dimensional model of corotating streams in the solar wind, 1, Theoretical foundations, J. Geophys. Res., 83, 5563, 1978.

Pizzo, V. J., A three-dimensional model of corotating streams in the solar wind, 2, Hydrodynamic streams, J. Geophys. Res., 85, 727, 1980.

Pizzo, V. J., A three-dimensional model of corotating streams in the solar wind, 3, Magnetohydrodynamic streams, J. Geophys. Res., 87, 4374, 1982.

Pizzo, V. J., Quasi-steady solar wind dynamics, in Solar Wind

Five, edited by M. Neugebauer, NASA CP-2280, pp. 675-691, 1983.

Smith, E. J., and J. H. Wolfe, Observations of interaction regions and corotating shocks between one and five AU: Pioneer 10 and 11, Geophys. Res. Lett., 3, 137, 1976.

Steinolfson, R. S., M. Dryer, and Y. Nakagawa, Numerical MHD simulation of interplanetary shock pairs, J. Geophys. Res., 80, 1223, 1975.

Volkmer, P. M., and F. M. Neubauer, Statistical properties of fast magnetoacoustic shock waves in the solar wind between 0.3 AU and 1 AU: Helios-1,2 observations, (preprint) submitted to Annales Geophysicae, 1984.

Whang, Y. C., A magnetohydrodynamic model for corotating interplanetary structures, J. Geophys. Res., 85, 2285, 1980.

Whang, Y. C., The forward-reverse shock pair at large heliocentric distances, J. Geophys. Res., 89, 7367, 1984.

Whang, Y. C., and T. H. Chien, Magnetohydrodynamic interaction of solar wind streams, J. Geophys. Res., 86, 3263, 1981.

Whang, Y. C., and L. F. Burlaga, Coalescence of two pressure waves associated with stream interactions, J. Geophys. Res., 90, 221, 1985.

Figure Captions

Figure 1. This plot shows the relative positions of the three spacecraft (Voyager 1, Voyager 2, and Pioneer 10) in a three months period starting November 1977 with reference to IMP-8 calculated using an average solar wind speed of 0.22 AU/day. The three spacecraft and IMP-8 were within 15 degrees apart in longitudes and within 5 degrees in latitudes.

Figure 2. This figure shows the hourly averages of the solar wind speed observed by IMP-8, Voyager-1, and Pioneer-10. Three large streams (A, B and C) were observed by IMP-8 at 1 AU and by Voyagers at 1.5 AU. This solar wind was observed by Pioneer-10 at 15.1 AU as a distinctly different structure consisting of four shocks FB, RA, FC, and RB.

Figure 3. The formation of a forward-reverse shock pair at the leading edge region of stream B involves a rather complicated process including formation, collision, and merging. This figure shows the computed profiles of the solar wind speed (the t, u -profiles) at the leading edge of stream B between 1 AU and 3 AU at an increment of 0.04 AU. At 3 AU the solar wind structure consists of two forward shocks and a reverse shock RB. Later on the two forward shocks also merged, and the leading edge region of stream B evolved into a simple shock pair (FB and RB) by 4 AU.

Figure 4. The flow speed profiles and the total pressure profiles show the evolution of stream B and its interaction with neighboring streams A and C. At 4 AU stream B evolved into a single interaction region bounded by a forward-reverse shock pair. The interactions regions associated with stream B and C merged at 9.52 AU as shock FC collided with RB, it again merged

with the interaction region associated with streams A at 11.43 AU as shock FB collided with shock RA.

Figure 5. The calculated trajectories of shocks in a frame of reference moving at a speed of 0.22 AU/day illustrate the relationship between the sequence of shocks (FB, RA, FC, and RB) observed by Pioneer-10 and the large interplanetary streams (A, B, and C) observed by IMP-8.

Figure 6. Shock RB is used as an example to illustrate how the state of a reverse shock may vary as it moves from 1 AU to 16 AU in 85 days. The shock strength grew rapidly during the initial formation process inside 2 AU. RB collided with a forward shock at 2.03 AU, merged with three other reverse shocks between 2.4 AU and 4 AU, collided with FC near 9.52 AU, then interacted with a contact surface near 14.5 AU.

Figure 7. Three large streams (A, B and C) were observed by Helios-1 near 0.6 AU in May 1980. The streams evolved into a distinctly different structure consisting of four shock waves arranged in a F-F-R-R sequence at 8.1 AU observed by Voyager-1 in June 1980.

Figure 8. A detailed plot of the profiles of the solar wind speed (the t, u -profiles) between 0.6 AU and 8.1 AU at an increment of 0.1 AU shows that several formation, merging and collision processes took place during the evolution of the three streams A, B, and C. The evolution process has a more complex history. At 8.1 AU the streams evolved into a sequence of four shocks FB, FC, RA, and RBC. The use of a quantitative nonlinear simulation model including shock merging process is crucial in the interpretation

of data obtained in the outer heliosphere.

Figure 9. The flow speed profiles and the total pressure profiles show the evolution of the interplanetary dynamical structure for the interaction of the three streams A, B, and C. Each merging or collision creates a significant change in the profiles of the total pressure. The interaction regions associated with streams A, B, and C have coalesced by 8.1 AU.

Figure 10. The calculated trajectories of shocks in a frame of reference moving at a speed of 0.22 AU/day provides a summary of all the interactions out to 8.1 AU. The plot explains the relationship between the sequence of shocks observed by Voyager-1 and the large interplanetary streams observed by Helios-1. The times at which the shocks were observed by Voyager-1 agree within 10% with those computed from the Helios-1 observations.

L. F. Burlaga, Laboratory for Extraterrestrial Physics, NASA-Goddard Space Flight Center, Greenbelt, MD 20771.

Y. C. Whang, Department of Mechanical Engineering, Catholic University of America, Washington, DC 20064.

POSITION OF SC (V1, V2, OR P10) RELATIVE TO IMP8

$$\Delta\phi = \phi_{SC} - \phi_{IMP8}$$

$$\Delta\theta = \theta_{SC} - \theta_{IMP8}$$

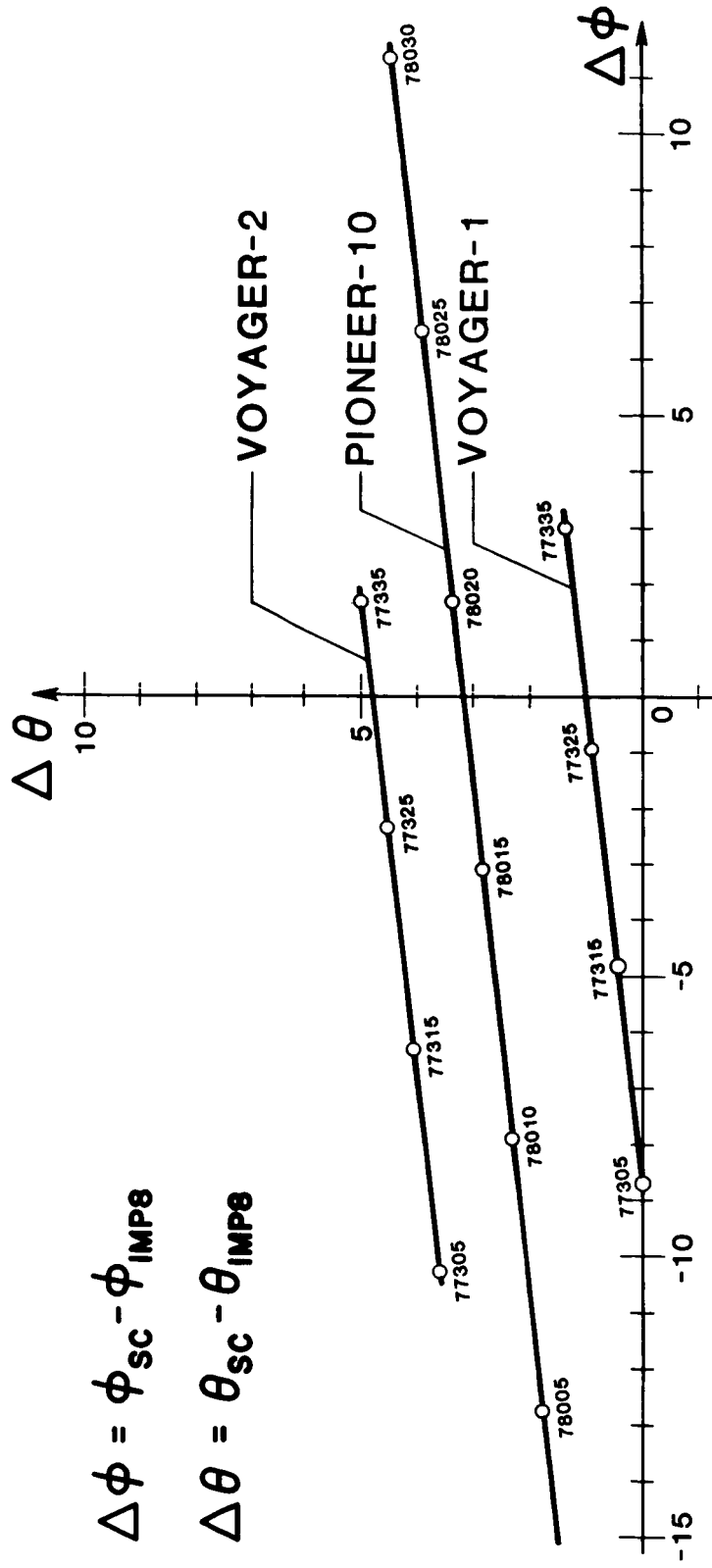


Figure 1

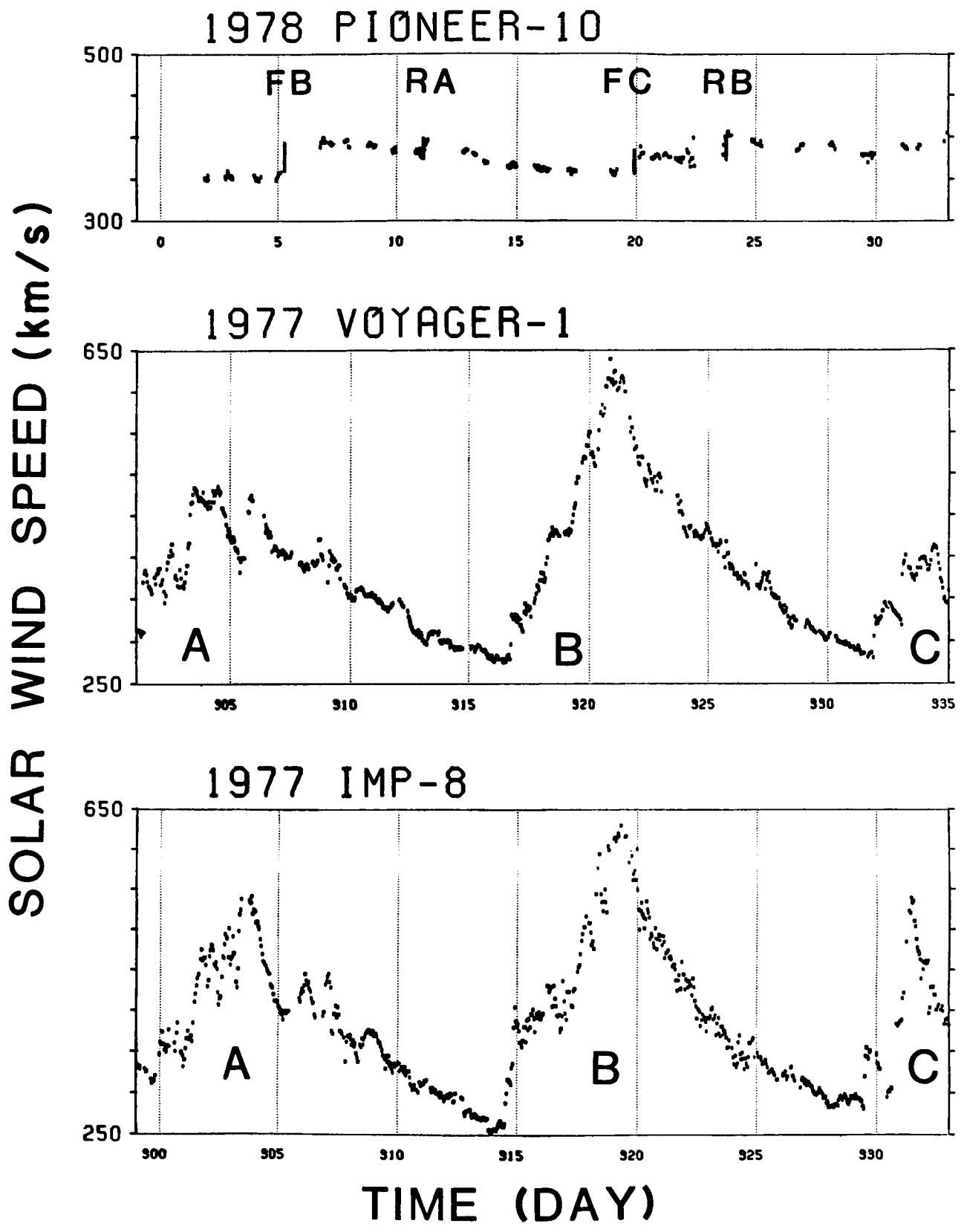


Figure 2

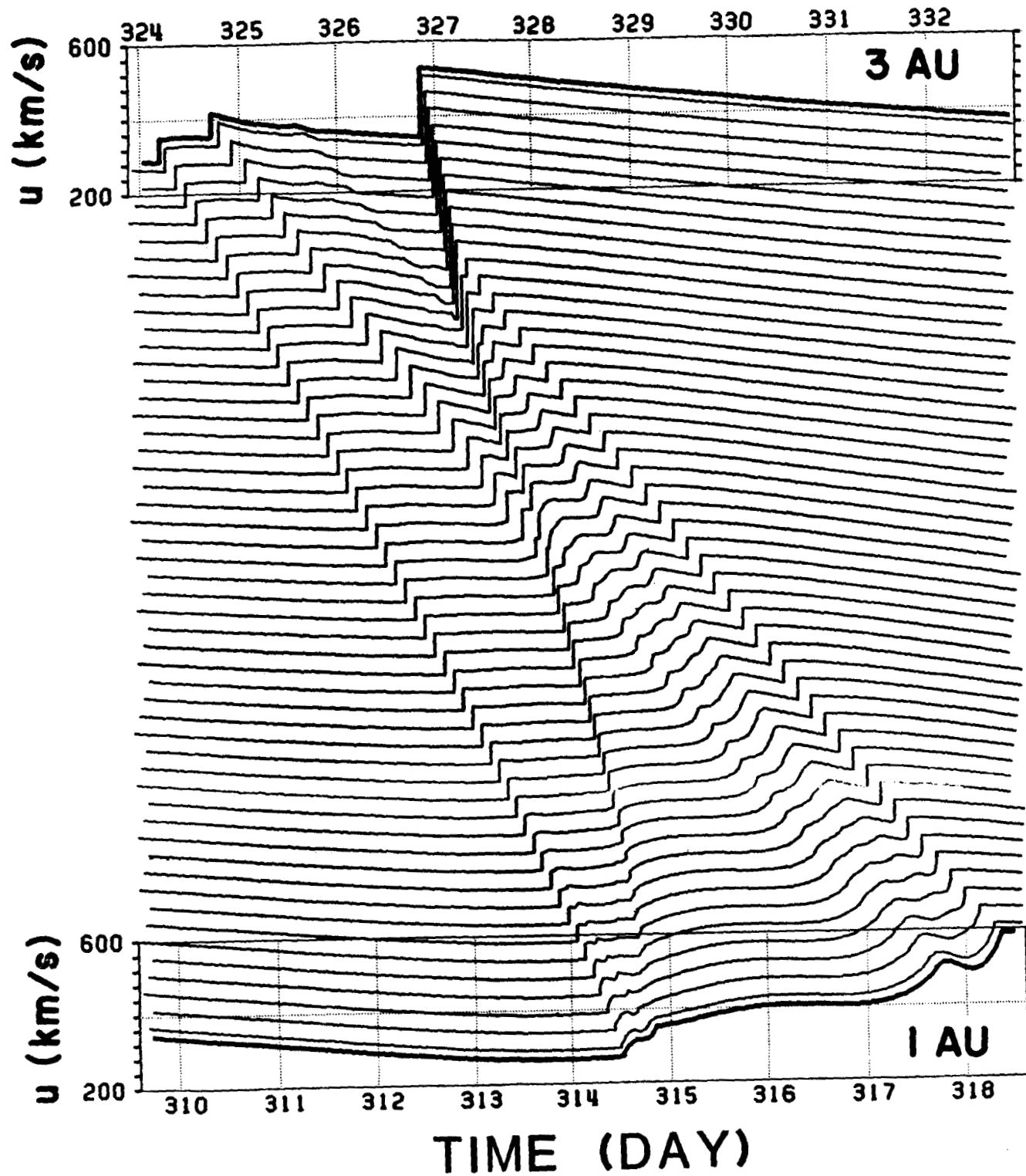


Figure 3

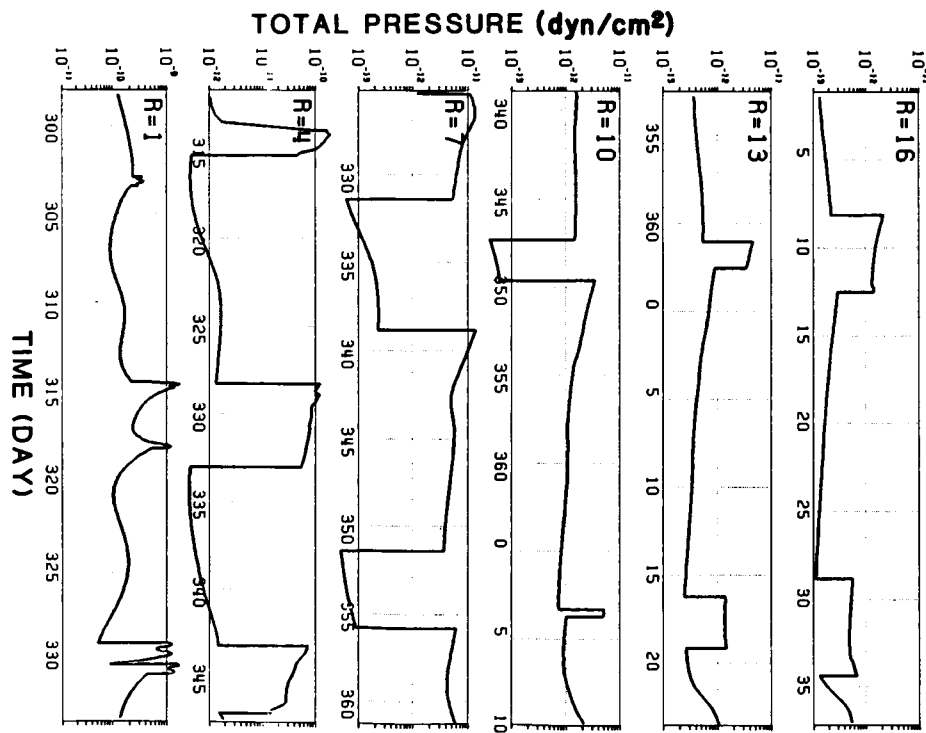
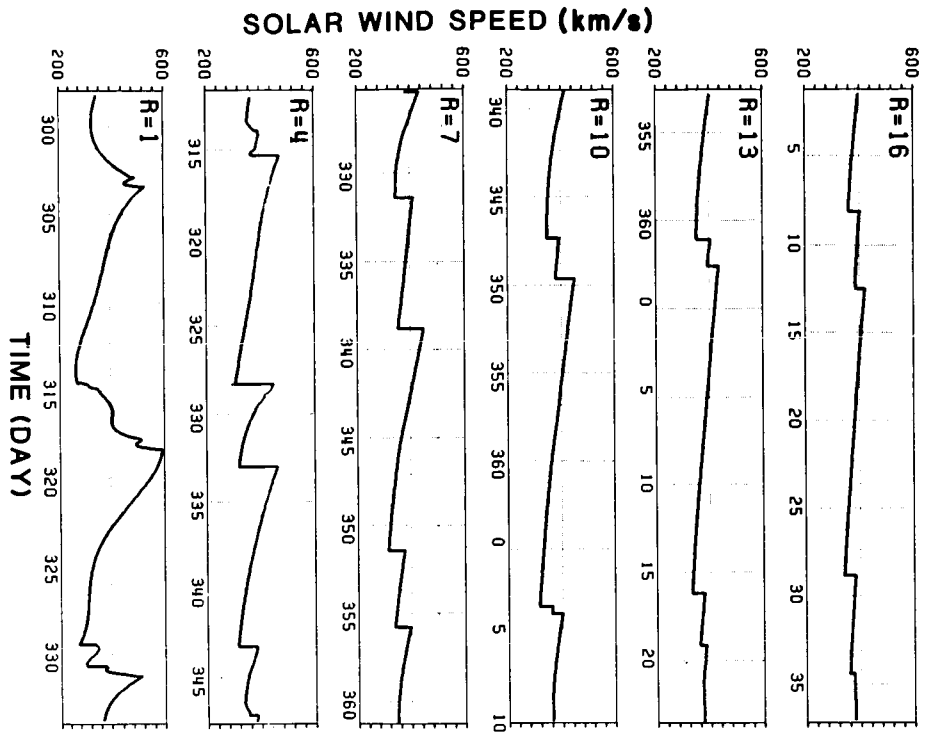


Figure 4

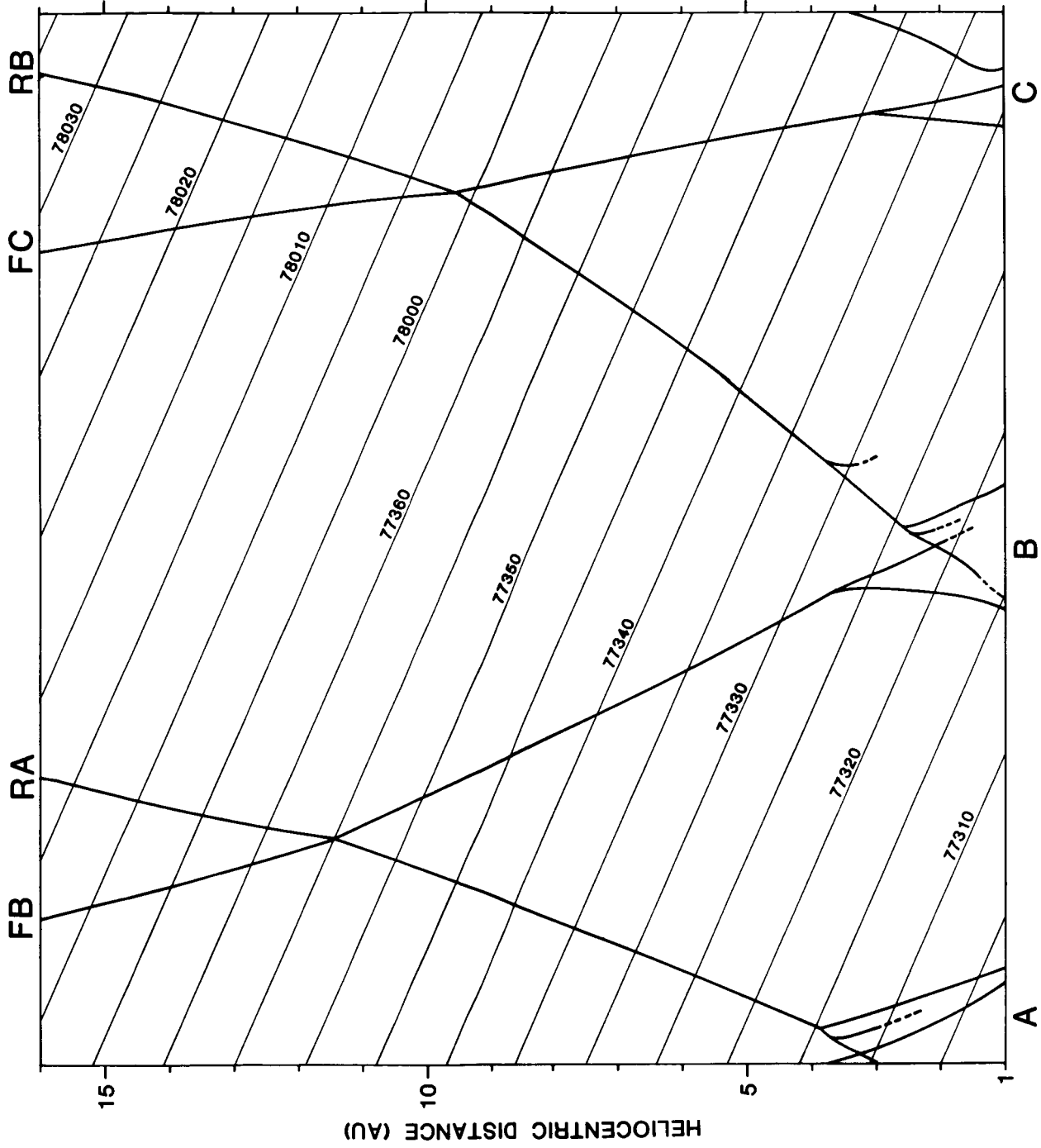
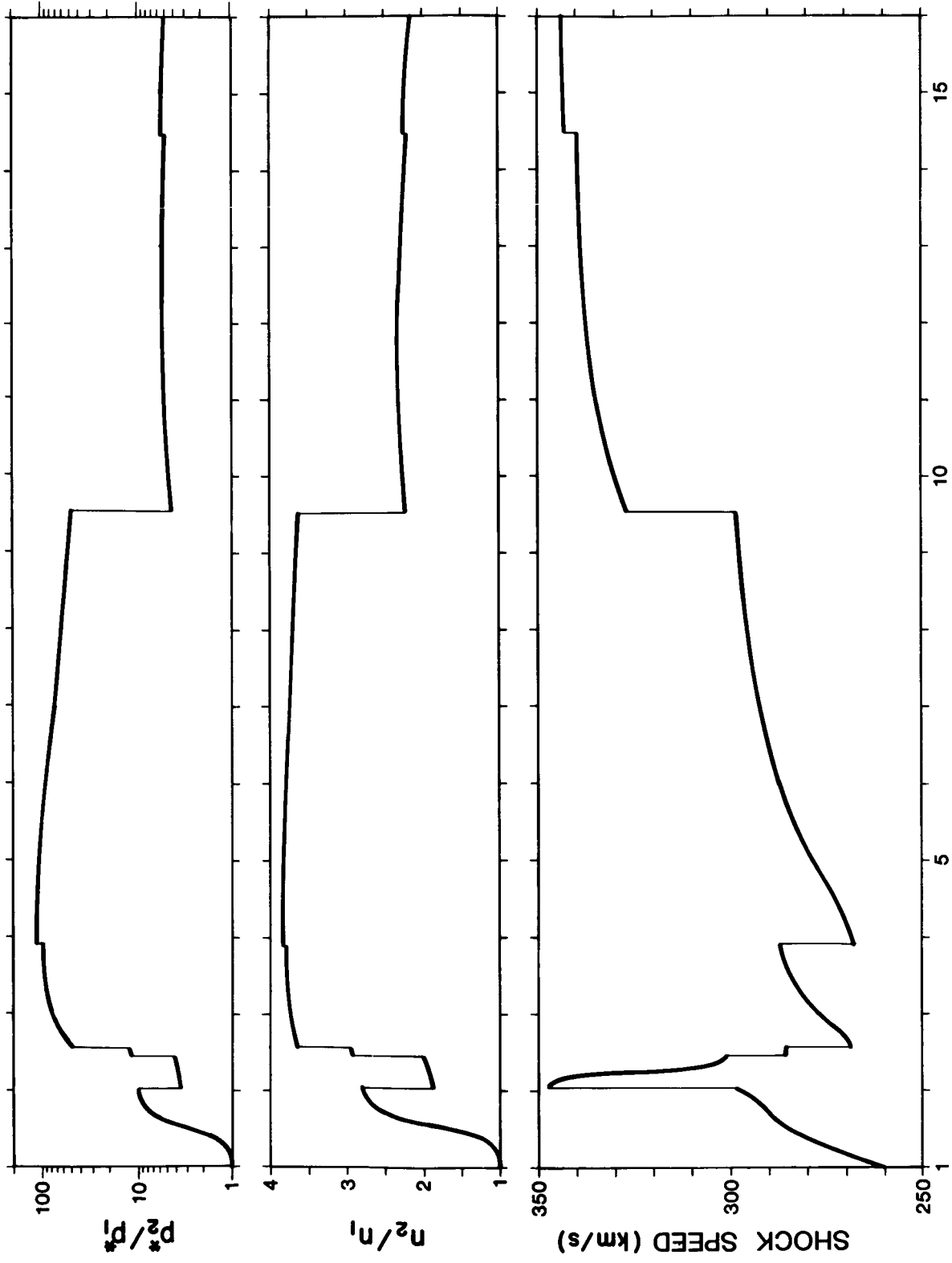


Figure 5



HELIOCENTRIC DISTANCE (AU)

Figure 6

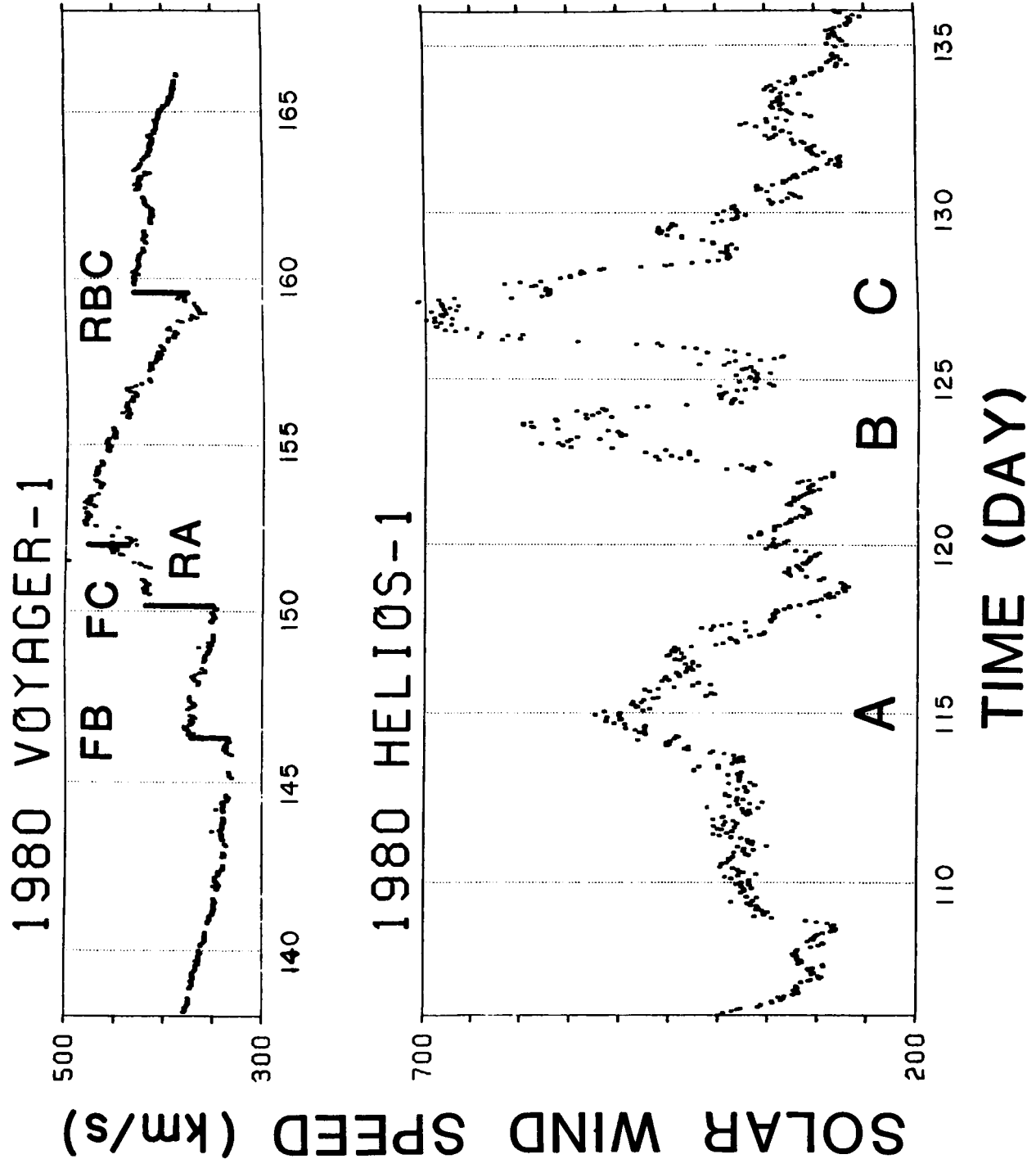


Figure 7

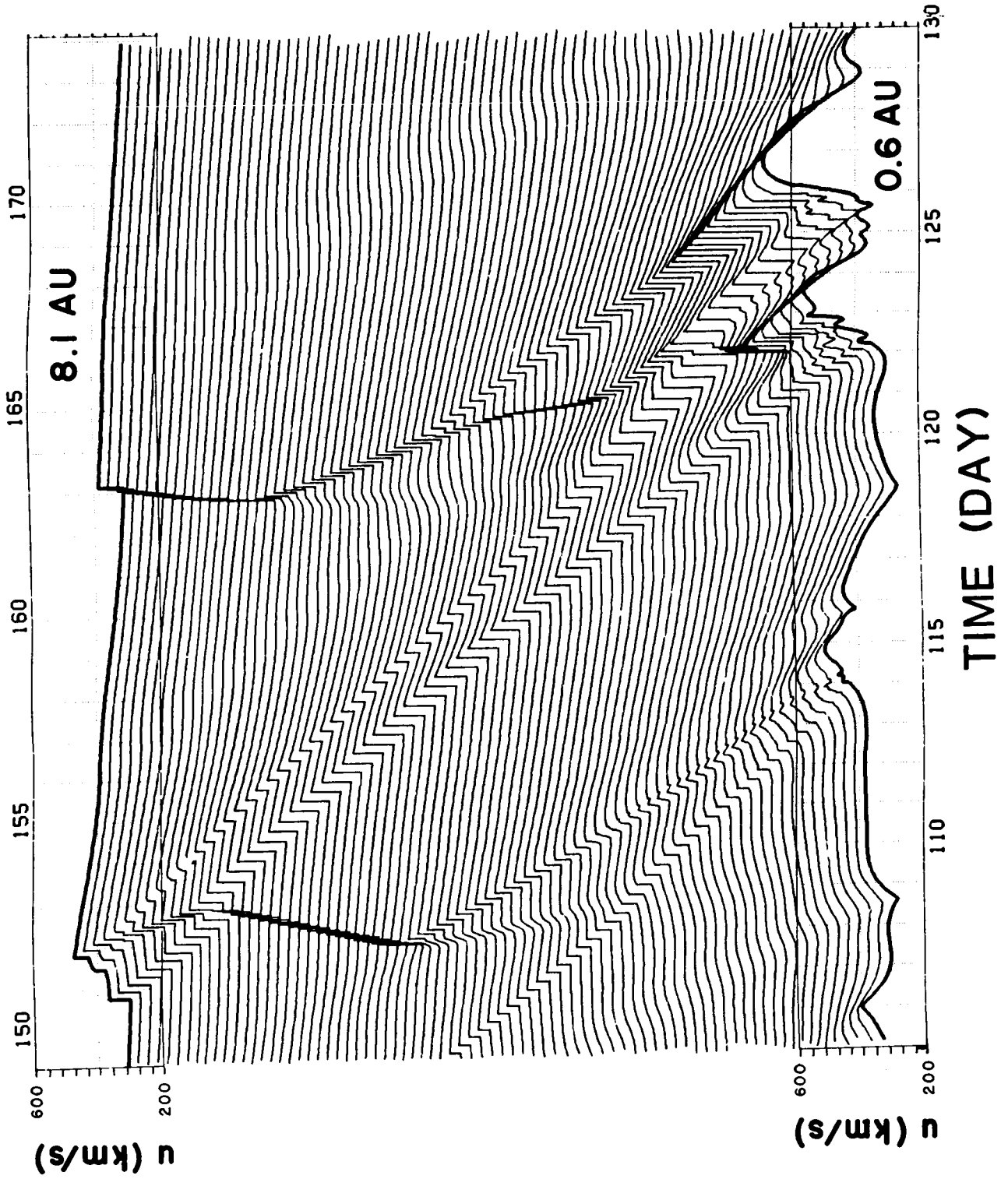


Figure 8

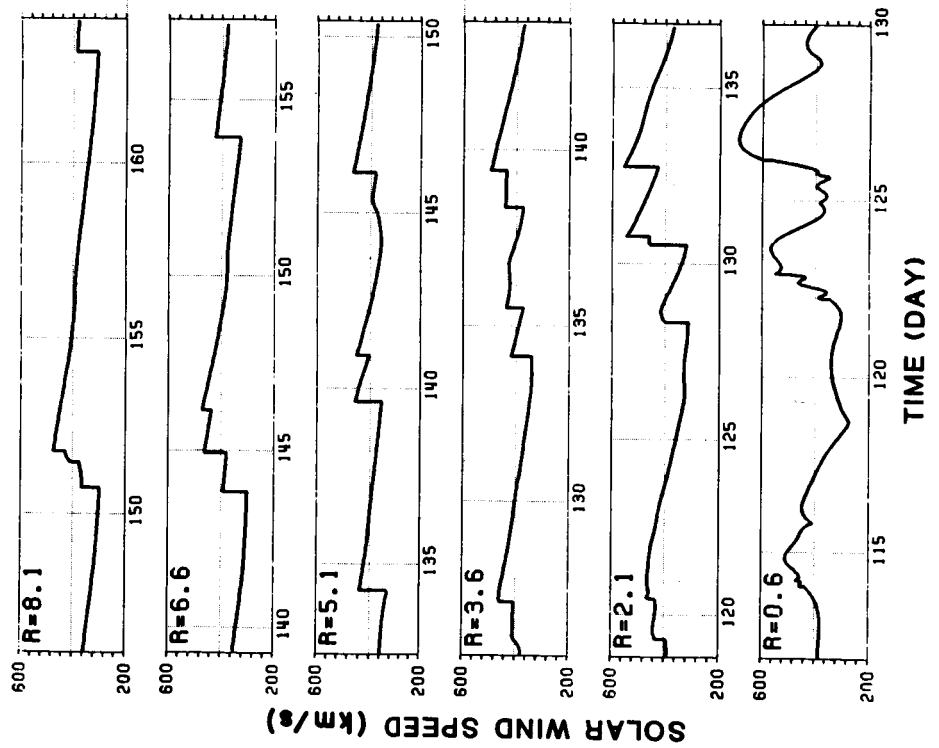
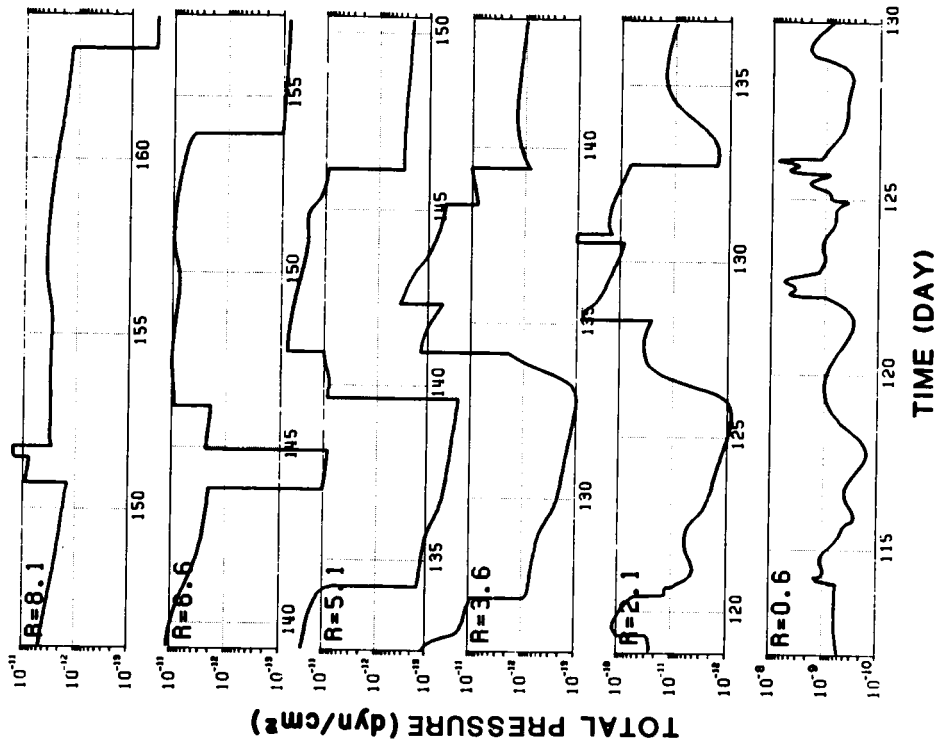


Figure 9

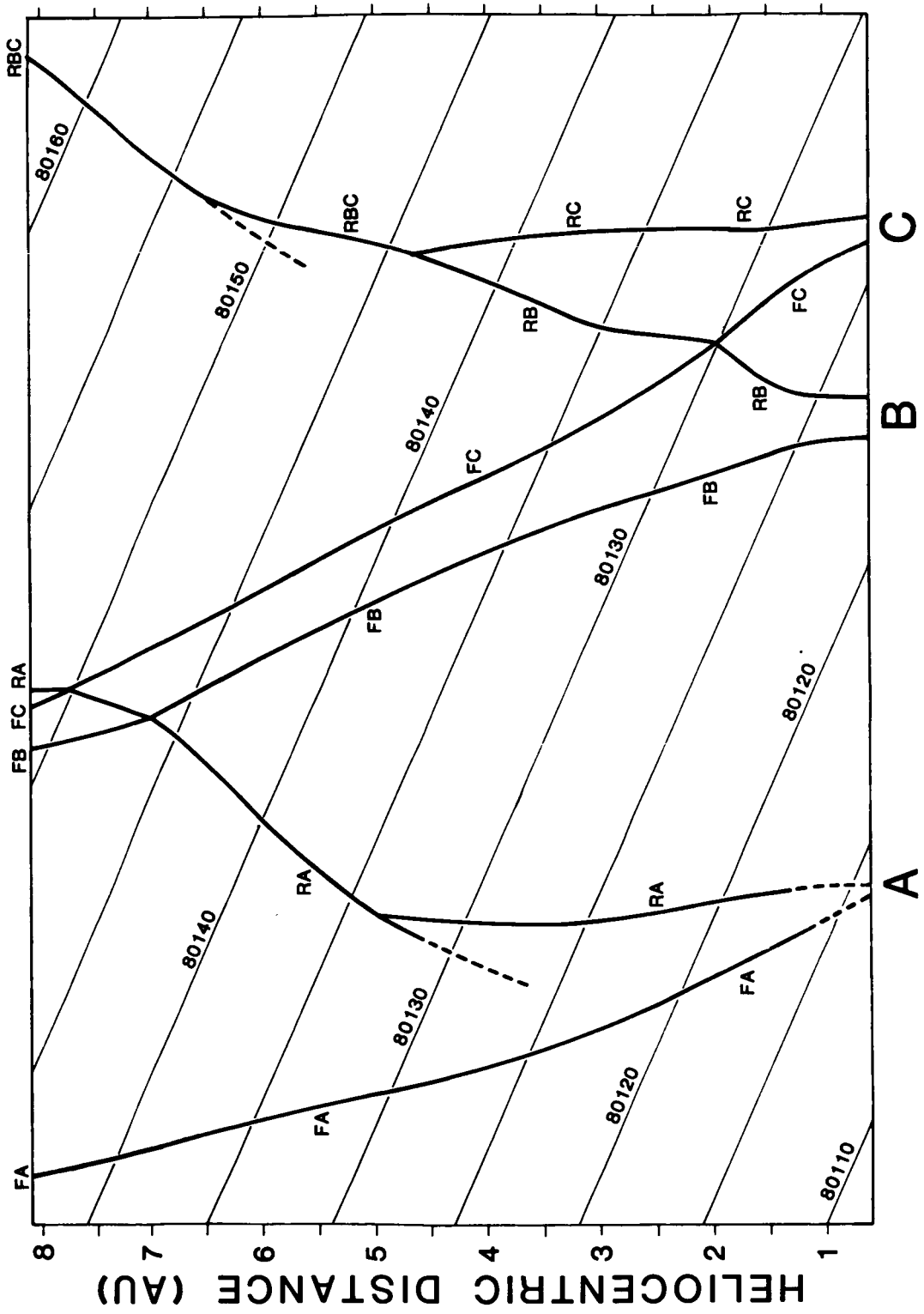


Figure 10

BIBLIOGRAPHIC DATA SHEET

1. Report No. TM 86192	2. Government Accession No.	3. Recipient's Catalog No.	
4. Title and Subtitle Evolution and Interaction of Large Interplanetary Streams		5. Report Date February 1985	
		6. Performing Organization Code	
7. Author(s) Y. C. Whang and L. F. Burlaga		8. Performing Organization Report No.	
9. Performing Organization Name and Address NASA/GSFC Laboratory for Extraterrestrial Physics Interplanetary Physics Branch, Code 692 Greenbelt, MD 20771		10. Work Unit No.	
		11. Contract or Grant No.	
		13. Type of Report and Period Covered Technical Memorandum	
12. Sponsoring Agency Name and Address		14. Sponsoring Agency Code	
		15. Supplementary Notes	
16. Abstract <u>SEE ATTACHED.</u>			
17. Key Words (Selected by Author(s)) Shocks, stream interactions, magnetic fields		18. Distribution Statement	
19. Security Classif. (of this report) U	20. Security Classif. (of this page) U	21. No. of Pages 41	22. Price*